

<http://ansinet.com/itj>

ITJ

ISSN 1812-5638

# INFORMATION TECHNOLOGY JOURNAL

**ANSI***net*

Asian Network for Scientific Information  
308 Lasani Town, Sargodha Road, Faisalabad - Pakistan

## Calibration Methods for 3D Thermo-sensing System

Tao Li and Kikuhito Kawasue

Faculty of Engineering, University of Miyazaki, 1-1, Gakuen Kibanadai-nishi, Miyazaki-shi, Japan

---

**Abstract:** Infrared (IR) thermography is device that can measure the distribution of infrared energy emitted from the surface of these objects. Since two-dimensional thermal images can be easily obtained without making contact with the object, the thermography has been used in fields such as agriculture, medicine, engineering and architecture. This study presents calibration methods that enable combining three-dimensional (3D) scanning technology with thermography. Three types of image measurement systems are introduced. The proposed systems can detect not only the 3D shape of a target object but also its temperature distribution. Application technology based on infrared thermography can make great strides in biological and medical fields by acquiring the 3D temperature distribution. In addition, a new Iterative Closest Point (ICP) algorithm is introduced. The feasibility of the proposed systems was confirmed by experiment.

**Key words:** Thermal image, calibration, three-dimensional, triangulation, thermography

---

### INTRODUCTION

All objects emit electromagnetic radiation. The position relationship between the absolute temperature of an object and the intensity and wavelength of the emitted radiation is defined by the Stefan-Boltzmann Law (Kateb *et al.*, 2009). Over the past 50 years, a large number of studies, particularly the correlation between temperature patterns and medical conditions in humans and animals, have been conducted (Watanabe *et al.*, 1998). In biomedical engineering, infrared thermography is an important measurement tool for evaluating the state of human health through careful analysis of skin surface temperatures (Speakman and Ward, 1998). Since thermal images can be easily obtained without making contact with an object, the thermography has been used in various fields, such as agriculture, medicine, engineering and architecture. However, since thermal images captured by infrared thermography are two dimensional, quantitative information, such as the 3D surface shape and the area, cannot be obtained.

In general, there are two types of non-contact methods, i.e., the passive stereo method (Matsubara, *et al.*, 2008) and the active light-section method (Ikeda, 2010) which can obtain quantitative information including the three-dimensional shape and the area. These measurement methods are widely used in the industrial production field. Specially, the technique is used for automatic position detection and automatic inspection of component shape in the production site. It is also an important technology with respect to

improvement of productivity and working efficiency in the production line. Many 3D scanners are commercially available. However, since the 3D scanner is a closed system with software, this makes thermography combine with the other device difficultly.

In recent years, acquiring 3D thermal data is useful for restoration work of building and prediction of risk after a disaster occurs. This study presents calibration methods which can be used to measure the 3D surface shape of a target object but also its temperature distribution. Three types of image measurement systems are introduced in this study. Experimental results show the feasibility of our systems.

### SYSTEMS SETTING

The proposed systems are established by combining the thermography with the 3D shape measurement device. The configuration of the proposed systems is shown in Fig. 1.

Three types of 3D shape measurement device have been developed. The first system is composed of a CCD camera and a slit laser projector. The laser projector equipped on a uniaxial stage is projected on the surface of an object. The laser streak appeared on the surface of the object is recorded by the CCD camera and the thermography. 3D coordinates of points on the target object are calculated by analyzing the laser streak. Then, thermal data can be allocated to the corresponding 3D position using Eq. 5. In order to measure the global 3D temperature distribution of a target object, it is necessary

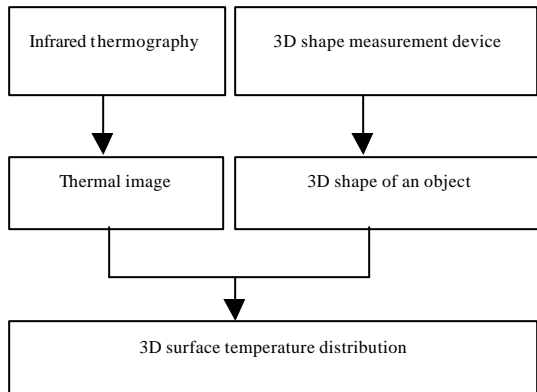


Fig. 1: Configuration of the proposed systems

to scan the slit laser. Here, a calibration black which some filaments were set at the each corner is used to allocate the temperature distribution data to the corresponding 3D position.

The second system is composed of a portable 3D instrument (Kinect sensor) and an infrared thermography which are unified. Since the portable 3D instrument consists of an infrared laser projector, an infrared camera and an RGB camera. 3D surface of a target object can be measured by triangulation process. In order to measure the global 3D shape data, a new iterative closest point (ICP) algorithm is introduced. Many studies about ICP technique have been reported (Rusinkiewicz and Levoy, 2001). However, these methods have some problems that it takes a long time to perform and error often occurs in the matching result. I proposed the IPC algorithm that can solve these problems. ICP algorithm by a multisport laser was proposed. The multisport laser is used to connect two point cloud data acquired by the Kinect sensor. Specially, it is necessary to extract the laser points in two cloud data. Connection of two point data can be realized by calculating the movement and the rotation angle of the laser points. Figure 2 shows two point data obtained at different position. Figure 3 shows connection of two point cloud data. The entire perimeter of a target object can be automatically measured by splicing the obtained shape data using the ICP algorithm. Therefore, global 3D temperature distribution of the target can be reconstructed.

The third system is composed of an image-capture unit (i.e., the CCD camera and the thermography device) and a laser projector which magnetic sensors are mounted on them. This enables portable scanning measurements to be performed since the magnetic sensors can detect the 3D position an orientation of the image-capture unit and the slit laser projector in real-time. 3D temperature

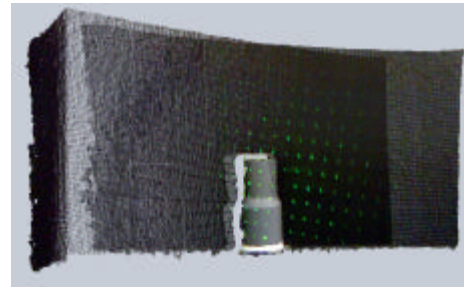


Fig. 2: Connection of two point cloud data

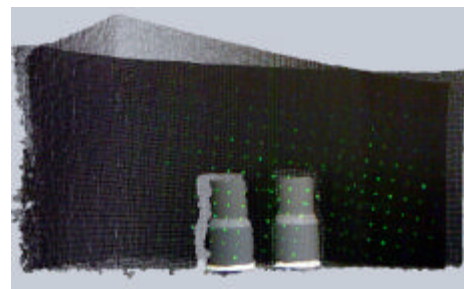


Fig. 3: Two point cloud data

distribution can be measured by maintaining the proper angle against the form of the target object. Occlusion problem which the back of a target object cannot be measured in the first proposed system can be solved.

In the study, in order to measure the 3D temperature distribution of a target object, calibrations of CCD camera and thermography are an important task since it influences the measurement accuracy and the allocation result between temperature data and the 3D shape data. Although a calibration process is very complicated and it is not usually unified in three-dimensional measurement system, suitable calibration methods for our systems are proposed in this study.

### MEASUREMENT PRINCIPLE

**Camera calibration:** In the first system and the third system, since a light-section method was used in these system, the 3D coordinates of points on the slit laser is calculated by estimating the intersection on the surface of the object between the laser plane and the vector from the focal point of the CCD camera. The relationship between the pixel coordinate of CCD camera  $(u, v)$  and the world coordinate  $(x, y, z)$  is formulated as follows (Tsai, 1987).

$$s \begin{bmatrix} u \\ v \\ 1 \end{bmatrix} = \begin{bmatrix} k_{11} & k_{12} & k_{13} & k_{14} \\ k_{21} & k_{22} & k_{23} & k_{24} \\ k_{31} & k_{32} & k_{33} & 1 \end{bmatrix} \cdot \begin{bmatrix} x \\ y \\ z \\ 1 \end{bmatrix} \quad (1)$$

Rearranging the equation, equation (1) can be written as follows:

$$\begin{bmatrix} x \\ y \end{bmatrix} = \begin{bmatrix} k_{31}u - k_{11} & k_{32}u - k_{12} \\ k_{31}v - k_{21} & k_{32}v - k_{22} \end{bmatrix} \cdot \begin{bmatrix} (k_{14} - u) & (k_{14}u - k_{13})z \\ (k_{24} - v) & (k_{14}v - k_{23})z \end{bmatrix} \quad (2)$$

where,  $k_{11}$  to  $k_{33}$  are parameters that consider the rotation, scale and displacement between pixel coordinates and world coordinates. It is called as camera calibration that estimates these parameters (Ueshiba and Tomita, 2003). These calibration parameters can be determined by inputting some corresponding coordinates between the pixel coordinates and the world coordinates using Eq. 1.

In the first system, since the slit laser moves along the uniaxial stage at 1mm interval, the z coordinate is indicated for the amount of movements of the uniaxial stage. The world coordinates of the measurement points can be calculated by Eq. 2.

In the second system, the 3D shape data is obtained by triangulation process. Specifically, in order to obtain the depth information, a constant pattern of speckles created by the laser source is projected onto the scene and recorded by the infrared camera. Then, this pattern is correlated against a reference pattern. The reference pattern is obtained by capturing a plane at a known distance from the sensor. As a speckle is projected on an object, the position of the speckle in the infrared image is shifted in the direction of the baseline between the laser projector and the perspective center of the infrared camera. All shifts of speckles are measured by the image correlation procedure which yields a disparity image. Each pixel at a distance to the sensor can be corrected from the corresponding disparity. The 3D shape data can be obtained using Eq. 3.

$$\begin{cases} x = \frac{d[u, v]}{f} \cdot ps \cdot (u - 320) \cdot 2.0 \cdot 0.001 [m] \\ x = \frac{d[u, v]}{f} \cdot ps \cdot (u - 240) \cdot 2.0 \cdot 0.001 [m] \\ z = d[u, v] \cdot 0.001 [m] \end{cases} \quad (3)$$

where, (u, v) are the pixel coordinates in the depth image and  $d[u, v]$  is the value of the brightness level in the

depth image and F is the focus of the infrared camera and ps is a constant parameter.

In the third system, since magnetic sensors can detect the 3D position an orientation of the image-capture unit and the slit laser projector in real time, 3D coordinates of points on the slit laser is integrated into the world coordinate system. However, in order to measure the 3D coordinates of points on the slit laser, it is necessary to determine the equation of the laser plane and the coordinate relationship between pixel coordinate of CCD camera and world coordinate in advance. The coordinate relationship between the pixel coordinate of CCD camera and the world coordinate can be determined by calibration process as Eq. 1. Equation of the laser plane is expressed as follows:

$$A \cdot x + B \cdot y + C \cdot z = 1 \quad (4)$$

where, A, B, C are constant parameters that can be determined by inputting 3 points. Therefore, the 3D shape data can be obtained by solving a simultaneous equation between Eq. 1 and 4.

**Thermography calibration:** In order to allocate the temperature data into the corresponding 3D shape data, it is necessary to calibrate the thermography since the corresponding position relationship between thermography coordinate and world coordinate need to determine in advance. As Eq. 1, the coordinate relationship between thermography coordinate (ut, vt) and world coordinate (x, y, z) is formulated as follows:

$$s \begin{bmatrix} u_t \\ v_t \\ 1 \end{bmatrix} = \begin{bmatrix} k_{11} & k_{12} & k_{13} & k_{14} \\ k_{21} & k_{22} & k_{23} & k_{24} \\ k_{31} & k_{32} & k_{33} & 1 \end{bmatrix} \cdot \begin{bmatrix} x \\ y \\ z \\ 1 \end{bmatrix} \quad (5)$$

where, it is called as thermography calibration that estimates the parameters ( $h_{11}$  to  $h_{33}$ ). These parameters can be determined by inputting some corresponding coordinates between the thermography coordinates and the world coordinates. Eq. 5 can be written as follows:

$$\begin{cases} u_t = \frac{(h_{11}x + h_{12}y + h_{13}z + h_{14})}{h_{31}x + h_{32}y + h_{33}z + 1} \\ v_t = \frac{(h_{21}x + h_{22}y + h_{23}z + h_{24})}{h_{31}x + h_{32}y + h_{33}z + 1} \end{cases} \quad (6)$$

Once parameters  $h_{11}$  to  $h_{33}$  and world coordinates of measurement points on the surface of a target object are

determined, the corresponding thermography coordinates can be calculated by Eq. 6. Therefore, the corresponding temperature data can be allocated to the reconstructed shape of a target object.

**EXPERIMENTS**

In the first system, since the size of an object projected in the image varies depending on the distance from the CCD camera to the object, the distance from the CCD camera to the object influences measurement accuracy. A cube block is used to evaluate the measurement accuracy. Precision evaluation was executed by taking a difference between the measured value and the intrinsic dimensions at various distances from 400 mm to 1200 mm at 100mm intervals. Figure 4 shows the measurement accuracy of the first proposed system. Measurement result of a human hand was introduced for one of the examples of the 3D temperature measurement. Figure 5 shows 2D thermal image. Red points appeared in thermal image are filaments which are used to match the

coordinates between the pixel coordinate and the world coordinate (or between the thermography coordinate and the world coordinate). The measurement result is shown in Fig. 6.

In the second system, since the size of the object appearing in the IR camera image also varies depending on distance from the Kinect sensor to the object, measurement accuracy for distance was carried out. To verify the relation between random error and the distance from the Kinect sensor, a flat board with scale was measured and the precision evaluation was carried out at various distances from 50-400-50 cm intervals. Figure 7 shows the measurement accuracy. Here, measurement result of a resin part is introduced for one of the examples of the 3D temperature measurement. Figure 8 shows the measurement result of the second proposed system.

In the third system, measurement accuracy is evaluated by changing the distance from the CCD camera

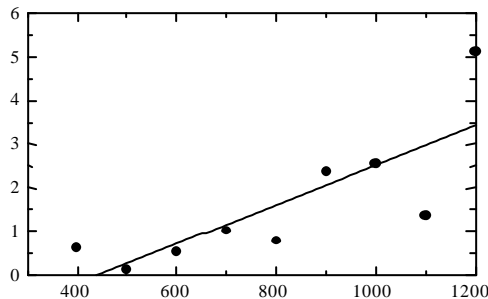


Fig. 4: Measurement accuracy

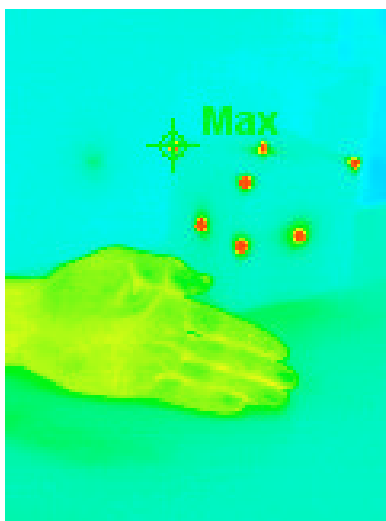


Fig. 5: 2D thermal image

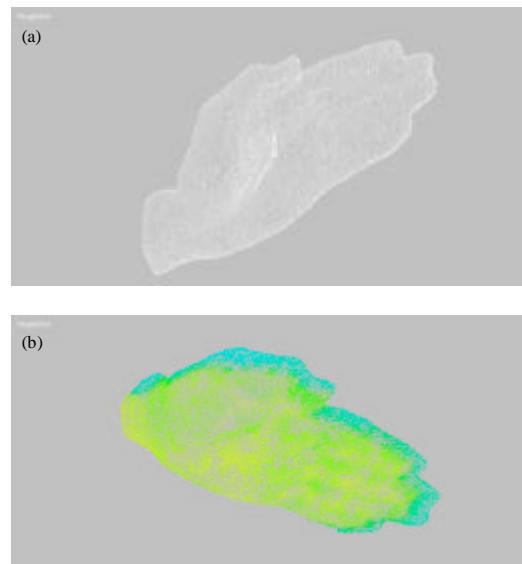


Fig. 6: Measurement result

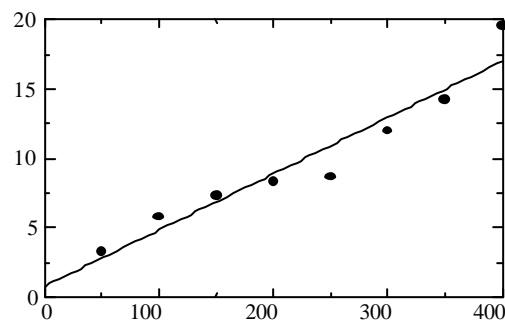


Fig. 7: Measurement accuracy for distance

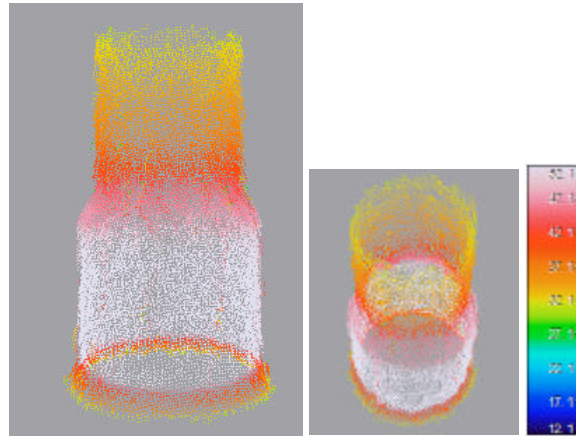


Fig. 8: Measurement result

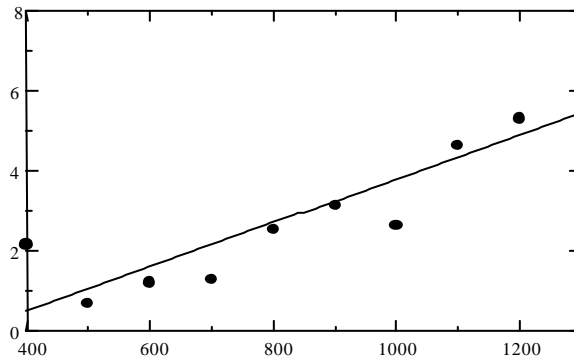


Fig. 9: Measurement accuracy for distance

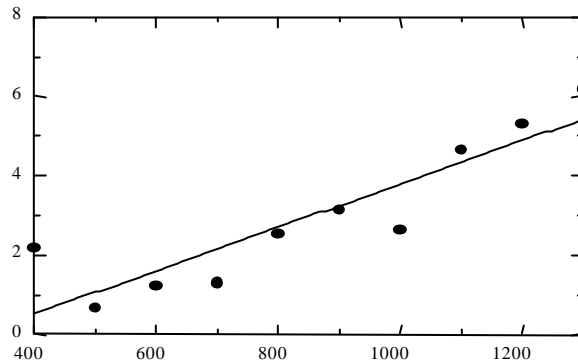


Fig. 10: Measurement accuracy for angle

to the object. To verify the relation between random error and the distance from CCD camera to the object, a plane scale board is measured. Precision evaluation was executed by taking the difference between the measured value and the intrinsic dimensions at various distances from 400-1300 mm at 100 mm intervals. Figure 9 shows the measurement accuracy of the third

proposed system. In addition, since the propose system is based on the principle of triangulation, the angle between the CCD camera and the laser projector influences the measurement accuracy. Therefore, the angle between the CCD camera and the laser slit was changed by 5 degree and the measurement accuracy was evaluated. Figure 10 shows the measurement

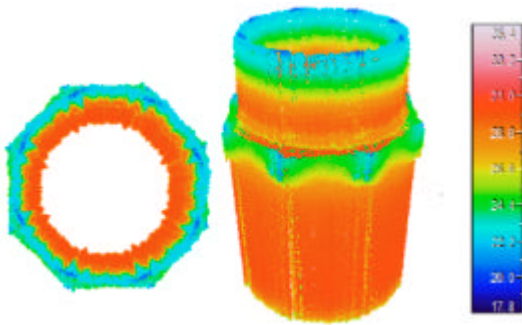


Fig. 11: Measurement result

accuracy for angle. Figure 11 shows the measurement result of a resin part.

### CONCLUSION

Calibration methods for 3D thermo-sensing system were introduced in the study. Based on the proposed mathematical model, the proposed systems could detect not only the 3D shape of an object but also its temperature distribution. Experimental results demonstrated the feasibility of our systems.

In the first system, the proposed system which can measure 3D temperature distribution of a target object was confirmed. However, since the system could not measure the back shape of the target object, the second system which can solve this occlusion problem was proposed. In this system, a new ICP algorithm was proposed. Although 2D thermal images recorded from different angles cannot be connected by each other, the 3D shape data can be connected using the algorithm. Therefore, the second system enabled 3D temperature distribution measurement of the entire object. However, since measurement accuracy of the second system was poor, the third system was proposed. Here, handy scanning measurement was realized by mounting two magnetic sensors on the image-capture unit and the laser projector.

In the study, since the proposed systems could detect the 3D shape and the temperature distribution of an object simultaneously, these systems can be a valuable model for current and future applications for modelling and simulating biological and physiological processes of the human body.

### REFERENCES

- Ikeda, M., 2010. High speed 3D range capture techniques. Inst. Inform. Television Eng. (ITE Tech. Rep.), 34: 9-14.
- Kateb, B., V. Yamamoto, C. Yu, W. Grundfest and J.P. Gruen, 2009. Infrared thermal imaging: A review of the literature and case report. NeuroImage, 47: T154-T162.
- Matsubara, K. and Y. Sasamoto *et al.*, 2008. Research on 3D shape measurement by stereo method. The Japan Society of Mechanical Engineers, pp: 27-28.
- Rusinkiewicz, S. and M. Levoy, 2001. Efficient variants of the ICP algorithm. Proceedings of the 3rd International Conference on 3D Digital Imaging and Modeling, May 28-Jun. 1, Quebec City, Canada, pp: 145-152.
- Speakman, J.R. and S. Ward, 1998. Infrared thermography: Principles and applications. Zoology, 101: 224-232.
- Tsai, R.Y., 1987. A versatile camera calibration technique for high-accuracy 3D machine vision metrology using off-the-shelf TV cameras and lenses. IEEE J. Robot. Autom., 3: 323-344.
- Ueshiba, T. and F. Tomita, 2003. Calibration of Multi-camera systems using planar patterns. Inform. Process. Soc. Japan, 44: 89-99.
- Watanabe, S. and Y. Yamanaka *et al.*, 1998. An exposure setup for *in vivo* studies to test biological effects in a head locally exposed to MW from a cellular telephone. Institute of Electronics, Information and Communication Engineers, pp: 15-22.